



Original scientific paper

## Electrochemical sensing of dopamine in the presence of serotonin using modified screen-printed carbon electrode

Somayeh Tajik<sup>1,✉</sup>, Fariba Garkani Nejad<sup>2</sup> and Hadi Beitollahi<sup>2</sup>

<sup>1</sup>Research Center for Tropical and Infectious Diseases, Kerman University of Medical Sciences, Kerman, Iran

<sup>2</sup>Environment Department, Institute of Science and High Technology and Environmental Sciences, Graduate University of Advanced Technology, Kerman, Iran

Corresponding Authors: ✉ [tajik\\_s1365@yahoo.com](mailto:tajik_s1365@yahoo.com)

Received: September 19, 2025; Accepted: November 5, 2025; Published: November 25, 2025

### Abstract

The Zr-based metal-organic framework (NH<sub>2</sub>-UiO-66(Zr))/graphene oxide (GO) nanocomposite was synthesized via a simple approach and used as a voltammetric sensing platform. By integrating NH<sub>2</sub>-UiO-66 (Zr) with GO, the resulting nanocomposite exhibits superior sensor performance due to synergistic effects. The sensor was fabricated using a straightforward drop-casting method, where a suspension of NH<sub>2</sub>-UiO-66 (Zr)/GO was applied to a screen-printed carbon electrode (NH<sub>2</sub>-UiO-66 (Zr)/GO/SPCE). The NH<sub>2</sub>-UiO-66 (Zr)/GO/SPCE sensor was then employed to determine dopamine (DA) using differential pulse voltammetry (DPV). The NH<sub>2</sub>-UiO-66 (Zr)/GO/SPCE sensor demonstrated a linear response to DA over a concentration range of 0.001 to 800.0 μM, with a high sensitivity of 0.1002 μA μM<sup>-1</sup>. Using the DPV method, a limit of detection (LOD) of 0.5 nM was achieved. It was further employed as a sensing platform for the simultaneous detection of DA and serotonin (STN). The DA and STN peak separation were 245 mV. The NH<sub>2</sub>-UiO-66 (Zr)/GO/SPCE sensor was successfully used to analyse DA and STN in a human urine sample, achieving satisfactory recovery rates of 97.8 to 104.2 %.

### Keywords

Neurotransmitters; electrochemical sensor; metal-organic framework; graphene oxide

### Introduction

As an essential neurotransmitter in the catecholamine family, dopamine (DA) is ubiquitously present throughout the brains of mammals. Its chemical structure is defined as 4-(2-aminoethyl) benzene-1,2-diol. DA is indispensable for the proper operation of several physiological systems, such as the central nervous, cardiovascular, hormonal and renal systems. Significant deviations from

normal DA levels, however, are recognized as a contributing factor in disorders like Parkinson's disease, Tourette's syndrome, schizophrenia, and the development of pituitary tumours. Consequently, quantifying DA concentrations in biological samples provides critical diagnostic insights for numerous pathologies, making it a central focus of contemporary biological investigation [1-3]. Serotonin (5-hydroxytryptamine) (STN), also known as 5-HT, is a monoamine neurotransmitter with a widespread presence in the brain. It exerts a considerable influence on a diverse array of pharmacological, physiological, and biological functions, including endocrine control, liver regeneration, muscle contraction, thermoregulation, and mood disorders such as depression [4-6]. Research has established that the DA and STN engage in reciprocal regulation, with each influencing the release of the other. Hence, the development of techniques for the simultaneous determination of DA and STN is of paramount importance, given their common presence and functional overlap in biological systems [7]. Numerous analytical techniques have been employed for the quantification of DA and STN, including chromatography [8], mass spectrometry [9], electrophoresis [10], fluorimetry and chemiluminescence-based assays [12,13]. Electrochemical techniques have emerged as a practical alternative for detecting redox-active species such as DA and STN, overcoming the common drawbacks of other methods. Namely, their high cost, prolonged analysis time, and large sample requirements [14].

Electrochemical techniques offer several distinct advantages, including high selectivity and sensitivity, straightforward miniaturization, low operational cost, and simplified sample preparation and handling. Due to their notable advantages, electrochemical sensors are the focus of extensive research aimed at advancing their use in fields such as food safety, medical diagnostics, and environmental monitoring [15-22]. The standard architecture of an electrochemical sensor is a three-electrode system, which can be readily fabricated on a chosen substrate using techniques such as patterning and printing. Screen-printed electrodes (SPEs) are planar instruments fabricated by sequentially printing layers of specialized ink onto a plastic, ceramic, or glass substrate. A variety of inks have been employed in electrode fabrication, particularly those based on carbon or noble metals, such as Ag, Au, and Pt. The principal advantages of these systems are their low cost, portability, operational simplicity, and reliable, compact design, which have led to their widespread adoption in biomedical, environmental, and analytical chemistry applications [23-28].

Bare electrodes are generally unsuitable for electrochemical detection, particularly for simultaneous analysis of DA and STN. Their limitations include susceptibility to surface fouling by molecules, poor sensitivity and selectivity in the presence of interferents, and the overlapping oxidation potentials of DA and STN, which prevent their resolution [29-31]. To circumvent these problems, one promising solution is the development and application of chemically modified electrodes. Modifying the electrode with various materials can dramatically enhance detection performance. Effective modifier materials are essential for significantly enhancing the selectivity and sensitivity of the electrochemical analysis. Therefore, the strategic design of these materials to possess high conductivity, a wealth of active sites, and a large surface area is crucial for maximizing this effect [32-35].

Considerable research interest has been focused on nanomaterials as advanced modifiers for chemically modified electrodes. Nanomaterials exhibit distinctive physicochemical, structural, and electrical properties due to their nanoscale size, which is distinct from that of bulk materials. This has established them as a prominent subject of study across multiple scientific disciplines [36-42]. Metal-organic frameworks (MOFs) represent a new class of crystalline and porous materials, synthesized by linking molecular building blocks of both metallic (metal clusters) and organic (ligand)

origin. These materials are attracting significant interest due to their permanent porosity, flexible structure, and greater surface area compared to other traditional porous materials, such as silica, zeolites, and activated carbon. Furthermore, the chemical landscape within these porous materials can be precisely engineered, allowing properties like polarity, functionality, and reactivity to be tailored in ways that are unattainable with conventional aluminosilicate zeolites. This remarkable versatility, with potential uses spanning from gas storage and separation to catalysis and pharmaceutical engineering, has positioned MOFs at the forefront of scientific inquiry [43-49]. MOFs have attracted significant attention in electrocatalysis, particularly for sensing platforms. This is largely due to their outstanding properties, including exceptionally large surface areas, tuneable pore architectures, and customizable surface chemistry. Specifically, a high density of accessible metal-active sites provides them with superior electrocatalytic performance. Furthermore, their extensive surface area and well-defined porous networks facilitate rapid and efficient transport of both analyte molecules and electrons. In recent studies,  $\text{NH}_2\text{-UiO-66}$ , a prominent member of the MOF family, has shown exceptional promise for electrochemical sensing platforms [50-53]. The utility of  $\text{NH}_2\text{-UiO-66}$  in electrochemical sensors, however, is hampered by its limited electrical conductivity. A promising route to overcome this challenge lies in combining the MOF with conductive components, thereby effectively improving electron-transfer kinetics and boosting sensing efficacy [54,55]. Among these, carbon nanomaterials such as graphene and carbon nanotubes are considered an ideal combination for constructing MOF composites. This preference stems from their straightforward synthesis, exceptional conductivity, and cost-effectiveness. The discovery of graphene, the first 2D material, introduced a substance with unparalleled versatility. Its single-layer sheets exhibit exceptional characteristics, such as ultra-high charge carrier mobility, superior electrical and thermal conductivity, optical transparency, and remarkable mechanical strength. Capitalizing on this unique profile, graphene derivatives like graphene oxide (GO) and reduced graphene oxide (rGO) have been extensively developed for use in sensing platforms [56-60].

In this research, an  $\text{NH}_2\text{-UiO-66 (Zr)}/\text{GO}$  nanocomposite was synthesized to create a highly effective modifier for a screen-printed carbon electrode (SPCE). The resulting modified electrode served as a sensitive analytical platform for the simultaneous detection of DA and STN. Due to the electrocatalytic activity of  $\text{NH}_2\text{-UiO-66 (Zr)}/\text{GO}$  nanocomposite, the created electrode ( $\text{NH}_2\text{-UiO-66 (Zr)}/\text{GO}/\text{SPCE}$ ) demonstrated high sensitivity for DA oxidation. Cyclic voltammetry (CV) was employed to investigate the electrochemical behaviour of DA at the surface of both the modified and bare electrodes. Voltammetric analysis revealed a substantially enhanced oxidation peak current for DA at the  $\text{NH}_2\text{-UiO-66 (Zr)}/\text{GO}/\text{SPCE}$  compared to the unmodified SPCE. The  $\text{NH}_2\text{-UiO-66 (Zr)}/\text{GO}/\text{SPCE}$  sensor displayed good sensitivity ( $0.1002 \mu\text{A}/\mu\text{M}$ ), linear concentration range ( $0.001$  to  $800.0 \mu\text{M}$ ) and good LOD ( $0.5 \text{ nM}$ ) for DA. Furthermore, the  $\text{NH}_2\text{-UiO-66 (Zr)}/\text{GO}/\text{SPCE}$  platform enabled significant peak separation, enabling simultaneous detection of DA and STN. The practical use of the  $\text{NH}_2\text{-UiO-66 (Zr)}/\text{GO}/\text{SPCE}$  sensor was successfully demonstrated by detecting DA and STN in a human urine sample, with highly satisfactory recovery rates.

## Experimental

### *Chemicals and apparatus*

All chemical reagents were obtained at the highest available commercial grade and used without further purification. All electrochemical investigations were conducted using a PGSTAT302N (Metrohm, The Netherlands). All experiments utilized disposable screen-printed carbon electrodes (SPCEs - model DRP-110) sourced from Metrohm-DropSens (Spain).

The  $\text{NH}_2\text{-UiO-66 (Zr)/GO}$  nanocomposite was synthesized as described in our previous work [61], and its FE-SEM image is shown in Figure 1.

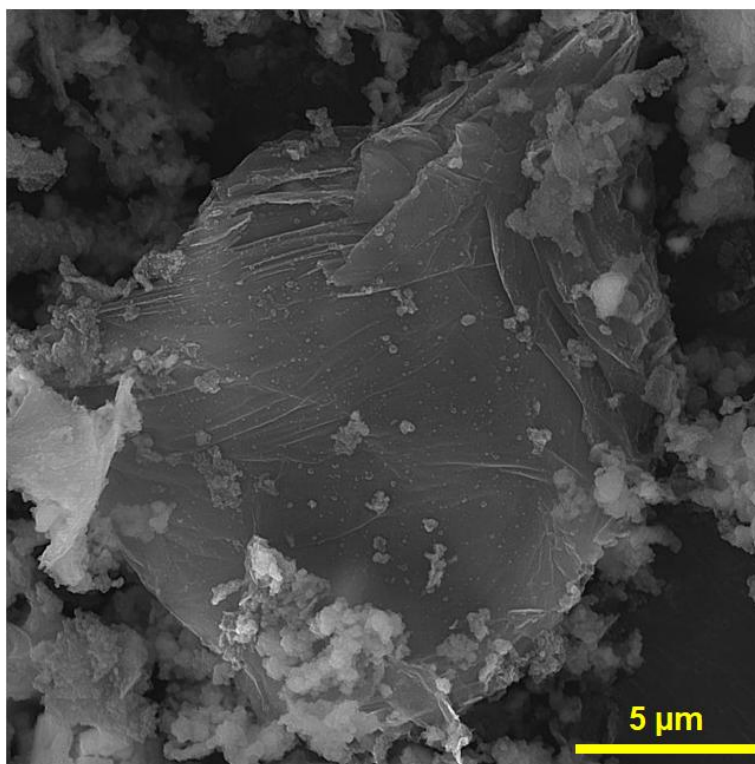


**Figure 1.** FE-SEM image of  $\text{NH}_2\text{-UiO-66 (Zr)/GO}$  nanocomposite

#### *Modification of SPCE with $\text{UiO-66-NH}_2$ MOF/GO nanocomposite*

The  $\text{NH}_2\text{-UiO-66 (Zr)/GO/SPCE}$  was fabricated by first preparing a homogeneous suspension of 0.5 mg  $\text{NH}_2\text{-UiO-66 (Zr)/GO}$  nanocomposite in deionized water (1.0 mL) *via* 40 min of sonication. A 4.0  $\mu\text{L}$  aliquot of this suspension was then drop-cast onto the SPCE surface and dried overnight at ambient temperature.

## **Results and discussion**

#### *Electrochemical behaviour of DA at the $\text{NH}_2\text{-UiO-66 (Zr)/GO/SPCE}$ and other sensing platforms*

The influence of PBS pH on the electrochemical response of DA was analysed by differential pulse voltammetry (DPV) across a range of pHs (2.0 to 9.0) at  $\text{NH}_2\text{-UiO-66 (Zr)/GO/SPCE}$ . The oxidation peak current of DA increased with pH, reaching a maximum at pH 7.0. Based on these results, a PBS at pH 7.0 was employed for all further experiments.

We performed CV experiments to study the capability of bare SPCE,  $\text{NH}_2\text{-UiO-66 (Zr)/SPCE}$ ,  $\text{GO/SPCE}$ , and  $\text{NH}_2\text{-UiO-66 (Zr)/GO/SPCE}$  in PBS (0.1 M, pH 7.0) containing 100.0  $\mu\text{M}$  DA with a scan rate of 50  $\text{mV s}^{-1}$ . As demonstrated in Figure 2, the electrochemical response of the bare SPCE to 100.0  $\mu\text{M}$  DA revealed weak redox peaks, characterized by a peak potential separation ( $\Delta E_p$ ) of 100 mV. The  $\text{NH}_2\text{-UiO-66 (Zr)/SPCE}$  demonstrated an  $I_{pa}$  enhancement of 11.5  $\mu\text{A}$  and an  $I_{pc}$  of -3.68  $\mu\text{A}$ . Furthermore, the  $\text{GO/SPCE}$  electrode exhibited higher redox peak currents than both the bare SPCE and the  $\text{NH}_2\text{-UiO-66 (Zr)/SPCE}$  platforms, demonstrating the high electrical conductivity and superior electrochemical performance of GO. The  $\text{NH}_2\text{-UiO-66 (Zr)/GO/SPCE}$  exhibits well-defined redox peaks with a  $\Delta E_p$  of 70 mV and a significant increase in the redox peak currents compared to the other SPCEs. These results indicate a positive influence of the modification of SPCE with the  $\text{NH}_2\text{-UiO-66 (Zr)/GO}$  nanocomposite.

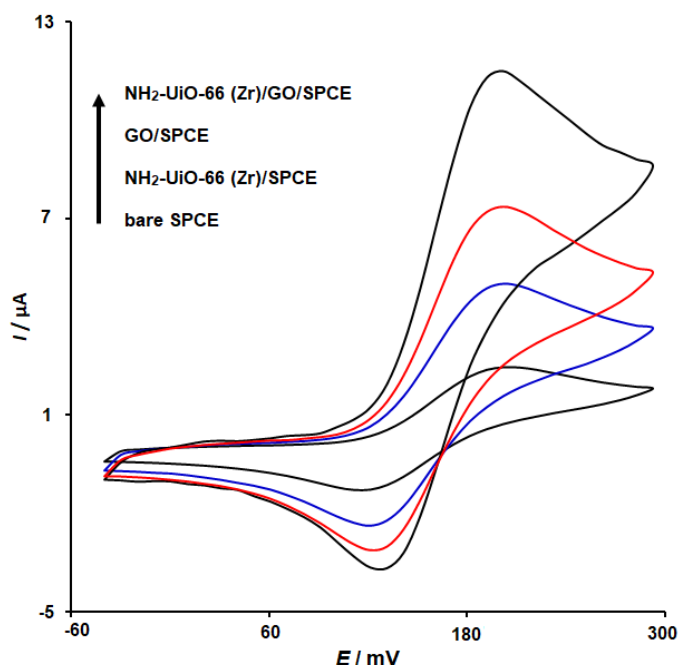


**Figure 2.** CV responses of bare SPCE,  $\text{NH}_2\text{-UiO-66 (Zr)/SPCE}$ ,  $\text{GO/SPCE}$ , and  $\text{NH}_2\text{-UiO-66 (Zr)/GO/SPCE}$  to DA ( $100.0 \mu\text{M}$ ) in PBS ( $0.1 \text{ M}$ ,  $\text{pH } 7.0$ ) (scan rate =  $50 \text{ mV s}^{-1}$ )

### Influence of scan rate

To investigate the reaction kinetics, CV was employed to examine the effect of scan rate ( $\nu$ ) on the redox processes of DA at the  $\text{NH}_2\text{-UiO-66 (Zr)/GO/SPCE}$ , varying the scan rates from 10 to  $300 \text{ mV s}^{-1}$ . As shown in Figure 3, the anodic and cathodic peak currents ( $I_{\text{pa}}$  and  $I_{\text{pc}}$ ) increase with the scan rate. Concurrently, a shift in peak potentials is observed. The inset in Figure 3 demonstrates that the redox peak currents exhibit a linear dependence on  $\nu^{1/2}$ . Suitable linear relationships were obtained, with the regression equations  $I_{\text{pa}} = 1.8999 \nu^{1/2} - 1.9868$  ( $R^2 = 0.9998$ ) and  $I_{\text{pc}} = -1.083 \nu^{1/2} + 2.5168$  ( $R^2 = 0.9992$ ), respectively. This indicates that the oxidation of DA at the  $\text{NH}_2\text{-UiO-66 (Zr)/GO/SPCE}$  is diffusion-controlled.

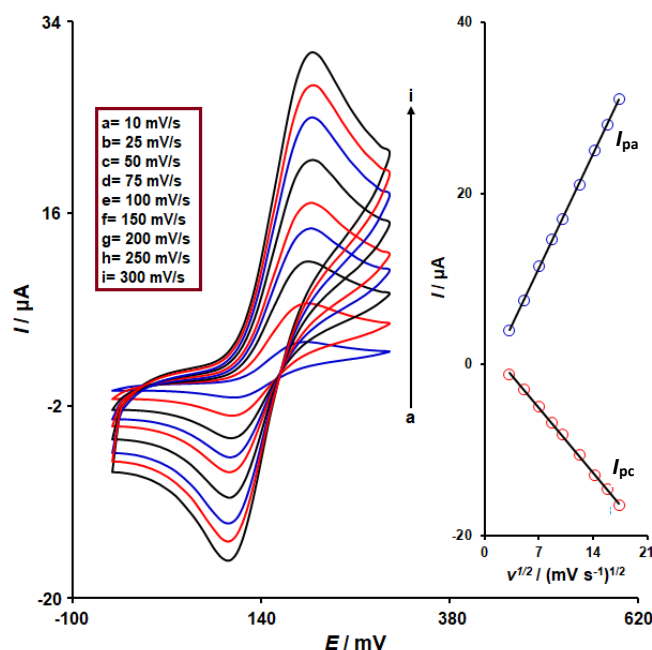


**Figure 3.** CV responses of  $\text{NH}_2\text{-UiO-66 (Zr)/GO/SPCE}$  to  $100.0 \mu\text{M}$  DA in PBS ( $0.1 \text{ M}$ ,  $\text{pH } 7.0$ ) at different scan rates from 10 to  $300 \text{ mV s}^{-1}$ . Inset: plots of peak currents ( $I_{\text{pa}}$  and  $I_{\text{pc}}$ ) vs.  $\nu^{1/2}$



### Chronoamperometric studies

The chronoamperometric analysis was also employed for the DA study at various concentrations, ranging from 0.1 to 1.6 mM, using NH<sub>2</sub>-UiO-66 (Zr)/GO/SPCE in PBS (0.1 M, pH 7.0) (Figure 4). The analysis was conducted using a constant potential of 230 mV at the NH<sub>2</sub>-UiO-66 (Zr)/GO/SPCE (as the working electrode). Under these mass-transport-controlled conditions, the chronoamperometric current for an electro-active species with a diffusion coefficient ( $D$ ) is defined via the Cottrell Equation (1):

$$I = nFACD^{1/2}\pi^{-1/2}t^{-1/2} \quad (1)$$

where  $D / \text{cm}^2 \text{s}^{-1}$  is the diffusion coefficient,  $A / \text{cm}^2$  is the electroactive surface area of the electrode and  $C / \text{mol cm}^{-3}$  is the bulk concentration of the analyte. The chronoamperometric current values were plotted against  $t^{-1/2}$  for diverse DA concentrations (Figure 4A). The slopes of the resulting linear fits were then plotted against the corresponding DA concentrations, as shown in Figure 4B. Using the slope from this latter plot in conjunction with the Cottrell equation, the average diffusion coefficient ( $D$ ) for DA was calculated to be  $3.6 \times 10^{-5} \text{ cm}^2 \text{s}^{-1}$ .

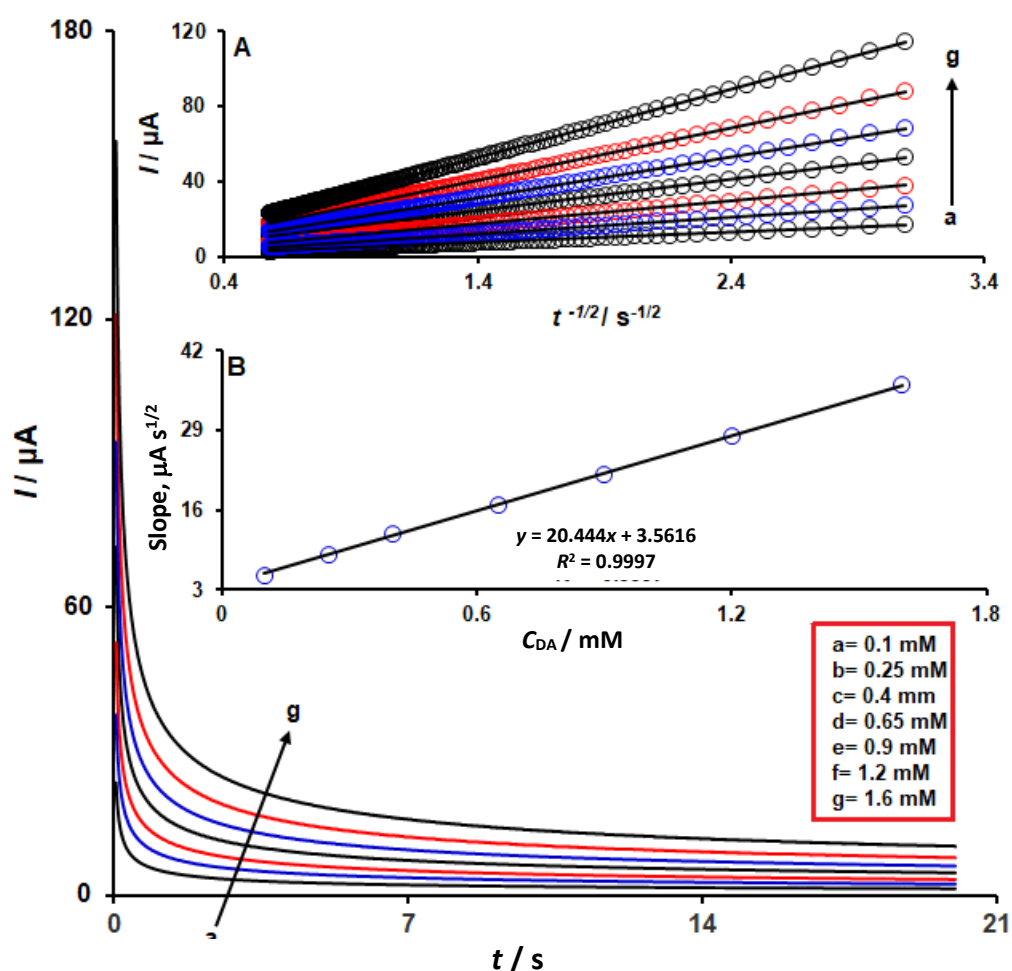


**Figure 4.** Chronoamperometric responses of NH<sub>2</sub>-UiO-66 (Zr)/GO/SPCE to DA at different concentrations from 0.1 to 1.6 mM in PBS (0.1 M, pH 7.0). Linear dependence of  $I$  on  $t^{-1/2}$  (Inset A) and linear dependence of the slope of the linear fits on DA concentration (Inset B)

### Quantitative measurements of dopamine at NH<sub>2</sub>-UiO-66 (Zr)/GO/SPCE sensor using differential pulse voltammetry

The DPV was utilized to evaluate the sensitivity of the NH<sub>2</sub>-UiO-66 (Zr)/GO/SPCE sensor by determining the linear detection range and LOD for DA. The DPV response for DA was recorded in 0.1 M PBS (pH 7.0), showing that the  $I_{pa}$  increased over a range of concentrations (Figure 5). The results

indicate that the  $I_{pa}$  increases linearly with DA concentration from 0.001 to 800.0  $\mu\text{M}$ . As shown in the inset of Figure 5, the calibration curve exhibits a strong linear relationship, described by the regression equation  $I_{pa} = 0.1002C_{DA} + 0.9212$  ( $R^2 = 0.9999$ ). Also, LOD was calculated to be 0.5 nM.

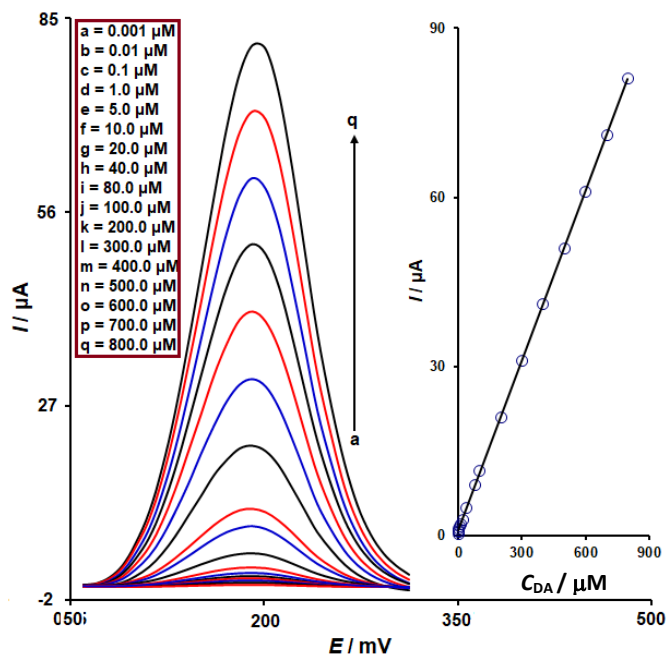


**Figure 5.** DPV responses of  $\text{NH}_2\text{-UiO-66 (Zr)/GO/SPCE}$  to DA at different concentrations from 0.001 to 800.0  $\mu\text{M}$  in PBS (0.1 M, pH 7.0). Inset: calibration plot of the  $I_{pa}$  response vs. DA concentration

#### Simultaneous determination of dopamine and serotonin at $\text{NH}_2\text{-UiO-66 (Zr)/GO/SPCE}$ sensor

To further illustrate the sensor's capability for simultaneous analysis, the concentrations of DA and STN were varied in a mixed solution, and the corresponding electrooxidation responses were monitored. Using DPV under optimal conditions, the  $\text{NH}_2\text{-UiO-66 (Zr)/GO/SPCE}$  sensor was used to simultaneously determine DA and STN in PBS (0.1 M, pH 7.0) (Figure 6).

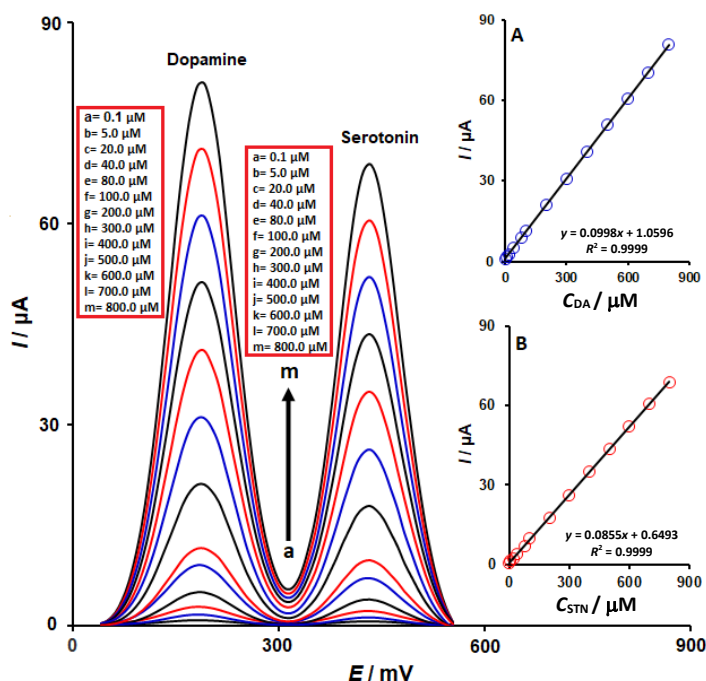


**Figure 6.** DPV responses of  $\text{NH}_2\text{-UiO-66 (Zr)/GO/SPCE}$  to various concentrations of DA (from 0.1 to 800.0  $\mu\text{M}$ ) and STN (from 0.1 to 800.0  $\mu\text{M}$ ) in PBS (0.1 M, pH 7.0). Insets: (A) calibration plots of  $I_{pa}$  response vs. DA concentration and (B)  $I_{pa}$  response vs. STN concentration

As shown in Figure 6, well-resolved peaks for DA and STN were observed, and the peak currents for each analyte exhibited a linear dependence on its concentration (Figure 6, Insets A and B). The sensitivity for DA determination in the presence of STN was determined to be 0.0995  $\mu\text{A}/\mu\text{M}$ . This value closely matches the sensitivity measured in pure DA solutions ( $0.1002 \mu\text{A} \mu\text{M}^{-1}$ , see Figure 5), confirming the method's selectivity.

*Application of the NH<sub>2</sub>-UiO-66 (Zr)/GO/SPCE platform for dopamine analysis in real sample*

To evaluate the validity and reliability of the NH<sub>2</sub>-UiO-66 (Zr)/GO/SPCE sensor in applicable applications, the determination of DA and STN in a human urine sample was achieved via DPV. To ensure accurate quantification in these matrices, the standard-addition method was used to determine DA and STN. Analytical results for DA and STN determination in the urine sample are provided in Table 1. As summarized in Table 1, the recovery rates for DA and STN ranged from 97.8 to 104.2 %, with associated relative standard deviations (RSDs) between 1.8 and 3.6 %. Therefore, the obtained recovery and RSD values confirm that the NH<sub>2</sub>-UiO-66 (Zr)/GO/SPCE sensor is both accurate and precise, demonstrating its strong potential for the determination of DA and STN in real samples.

**Table 1.** Analysis of urine sample for DA and STN determination by NH<sub>2</sub>-UiO-66 (Zr)/SPCE sensing platform (n = 5)

Sample	Added concentration, $\mu\text{M}$		Found concentration, $\mu\text{M}$		Recovery, %		RSD, %	
	DA	STN	DA	STN	DA	STN	DA	STN
Human urine	0	0	-	-	-	-	-	-
	5.0	4.0	4.9	4.1	98.0	102.5	3.6	1.8
	7.0	6.0	7.3	5.9	104.2	98.3	1.9	3.0
	9.0	8.0	8.8	8.3	97.8	103.7	2.4	2.3
	11.0	10.0	11.1	10.1	100.9	101.0	2.7	2.8

**Conclusion**

In summary, this research presents a readily fabricated voltammetric sensor utilizing an NH<sub>2</sub>-UiO-66 (Zr)/GO nanocomposite to modify a SPCE. The composite material synergistically combines the tunable porosity and excellent surface area of the NH<sub>2</sub>-UiO-66 (Zr) MOF with the superior conductivity of GO, creating an electrocatalytic platform that enhances electron transfer and provides abundant active sites. The developed sensor demonstrated excellent performance for the detection of DA, exhibiting a wide linear detection range, a low LOD, and good sensitivity. The NH<sub>2</sub>-UiO-66 (Zr)/GO/SPCE platform provided well-separated, well-defined voltammetric peaks for the oxidation of DA and STN, demonstrating its excellent suitability for simultaneous detection and practical sensing. Its practical use was successfully validated by accurate analysis of human urine, with satisfactory recovery rates, confirming its potential for reliable use in complex real-world matrices.

**Acknowledgement:** This study was financially supported by the Research Center of Tropical and Infectious Diseases, Kerman University of Medical Sciences, Kerman, Iran (grant number 404000066 and research ethics committee code of IR.KMU.REC.1404.026).

**Conflict of interest:** The authors have no conflict of interest.

**References**

[1] R. N. Goyal, V. K. Gupta, M. Oyama, N. Bachheti, Gold nanoparticles modified indium tin oxide electrode for the simultaneous determination of dopamine and serotonin: application in pharmaceutical formulations and biological fluids, *Talanta* **72** (2007) 976-983.  
<https://doi.org/10.1016/j.talanta.2006.12.029>



- [2] S. P. Nayak, V. Prathyusha, J. K. Kumar, Eco-friendly surface modification of oxidized carbon nanotubes with curcumin for simultaneous electrochemical detection of dopamine and serotonin, *Materials Chemistry and Physics* **287** (2022) 126293. <https://doi.org/10.1016/j.matchemphys.2022.126293>
- [3] A. Abbaspour, A. Noori, A cyclodextrin host–guest recognition approach to an electrochemical sensor for simultaneous quantification of serotonin and dopamine, *Biosensors and Bioelectronics* **26** (2011) 4674–4680. <https://doi.org/10.1016/j.bios.2011.04.061>
- [4] M. Bonet-San-Emeterio, A. González-Calabuig, M. del Valle, Artificial neural networks for the resolution of dopamine and serotonin complex mixtures using a graphene-modified carbon electrode, *Electroanalysis* **31(2)** (2019) 390–397. <https://doi.org/10.1002/elan.201800525>
- [5] J. Wei, J. B. He, S. Q. Cao, Y. W. Zhu, Y. Wang, G. P. Hang, Enhanced sensing of ascorbic acid, dopamine and serotonin at solid carbon paste electrode with a nonionic polymer film, *Talanta* **83** (2010) 190–196. <https://doi.org/10.1016/j.talanta.2010.09.005>
- [6] H. S. Han, H. K. Lee, J. M. You, H. Jeong, S. Jeon, Electrochemical biosensor for simultaneous determination of dopamine and serotonin based on electrochemically reduced GO-porphyrin, *Sensors and Actuators B: Chemical* **190** (2014) 886–895. <https://doi.org/10.1016/j.snb.2013.09.022>
- [7] S. Deepa, B. K. Swamy, K. V. Pai, Electrochemical sensing performance of citicoline sodium modified carbon paste electrode for determination of dopamine and serotonin, *Materials Science for Energy Technologies* **3** (2020) 584–592. <https://doi.org/10.1016/j.mset.2020.06.001>
- [8] K. E. Hubbard, A. Wells, T. S. Owens, M. Tegen, C. H. Fraga, C. F. Stewart, Determination of dopamine, serotonin, and their metabolites in pediatric cerebrospinal fluid by isocratic high performance liquid chromatography coupled with electrochemical detection, *Biomedical Chromatography* **24** (2010) 626–631. <https://doi.org/10.1002/bmc.1338>
- [9] F. Schumacher, S. Chakraborty, B. Kleuser, E. Gulbins, T. Schwerdtle, M. Aschner, J. Bornhorst, Highly sensitive isotope-dilution liquid-chromatography–electrospray ionization–tandem-mass spectrometry approach to study the drug-mediated modulation of dopamine and serotonin levels in *Caenorhabditis elegans*, *Talanta* **144** (2015) 71–79. <https://doi.org/10.1016/j.talanta.2015.05.057>
- [10] H. Fang, M. L. Pajski, A. E. Ross, B. J. Venton, Quantitation of dopamine, serotonin and adenosine content in a tissue punch from a brain slice using capillary electrophoresis with fast-scan cyclic voltammetry detection, *Analytical Methods* **5** (2013) 2704–2711. <https://doi.org/10.1039/C3AY40222C>
- [11] T. Yoshitake, J. Kehr, K. Todoroki, H. Nohta, M. Yamaguchi, Derivatization chemistries for determination of serotonin, norepinephrine and dopamine in brain microdialysis samples by liquid chromatography with fluorescence detection, *Biomedical Chromatography* **20** (2006) 267–281. <https://doi.org/10.1002/bmc.560>
- [12] Y. Lan, F. Yuan, T. H. Fereja, C. Wang, B. Lou, J. Li, G. Xu, Chemiluminescence of lucigenin/riboflavin and its application for selective and sensitive dopamine detection, *Analytical Chemistry* **91** (2018) 2135–2139. <https://doi.org/10.1021/acs.analchem.8b04670>
- [13] M. Kong, P. Jin, W. Wei, W. Wang, H. Qin, H. Chen, J. He, Covalent organic frameworks (COF-300-AR) with unique catalytic performance in luminol chemiluminescence for sensitive detection of serotonin, *Microchemical Journal* **160** (2021) 105650. <https://doi.org/10.1016/j.microc.2020.105650>
- [14] T. Joseph, J. Thomas, T. Thomas, N. Thomas, Selective nanomolar electrochemical detection of serotonin, dopamine and tryptophan using TiO<sub>2</sub>/RGO/CPE–influence of reducing agents, *New Journal of Chemistry* **45** (2021) 22166–22180. <https://doi.org/10.1039/D1NJ03697A>

- [15] H. Beitollahi, S. Tajik, M. R. Aflatoonian, A. Makarem, Glutathione detection at carbon paste electrode modified with ethyl 2-(4-ferrocenyl-[1,2,3] triazol-1-yl) acetate, ZnFe<sub>2</sub>O<sub>4</sub> nano-particles and ionic liquid, *Journal of Electrochemical Science and Engineering* **12** (2022) 209-217. <https://doi.org/10.5599/jese.1230>
- [16] A. Nagdalian, A. Yurievich Chernov, I. Rzhepakovsky, E. Shaposhnikov, I. Baklanov, S. Povetkin, A. Blinov, V. Varavka, A.A. Jaloob Aljanaby, A. Al Kafi, Simultaneous electrochemical analysis of epinephrine and folic acid, *Journal of Environmental and Bioanalytical Electrochemistry* **1** (2025) 143-150. <https://doi.org/10.48309/JEBE.2025.510683.1015>
- [17] L. Jia, Z. Lei, N. Zare, T. Wu, M. Ghalkhani, L. Wan, Y. Xu, Ti<sub>3</sub>C<sub>2</sub> MXene-enhanced electrochemical biosensors for prostate-specific antigen (PSA) detection in prostate cancer, *Journal of Nanostructure in Chemistry* **15** (2025) 152502. <https://doi.org/10.57647/jnsc.2025.1501.02>
- [18] R. Razavi, F. Garkani Nejad, S. A. Ahmadi, H. Beitollahi, Synthesis of ZnO@TiO<sub>2</sub> nanoparticles and its application to construct an electrochemical sensor for determination of hydrazine, *Electrochemistry Communications* **159** (2024) 107639. <https://doi.org/10.1016/j.elecom.2023.107639>
- [19] S. Z. Mohammadi, F. Mousazadeh, Novel strategy for hematoxylin electrochemical quantification based on screen printed electrode modified with graphene-CoS<sub>2</sub> nanocomposite, *Journal of Environmental and Bioanalytical Electrochemistry* **1** (2025) 135-142. <https://doi.org/10.48309/jebe.2025.507370.1012>
- [20] Z. Taleat, M. M. Ardakani, H. Naeimi, H. Beitollahi, M. Nejati, H. R. Zare, Electrochemical behavior of ascorbic acid at a 2,2'-[3,6-dioxo-1,8-octanediy]bis (nitriloethylidyne)]-bis-hydroquinone carbon paste electrode, *Analytical Sciences* **24** (2008) 1039-1044. <https://doi.org/10.2116/analsci.24.1039>
- [21] O. E. Fayemi, A. S. Adekunle, E. E. Ebenso, Electrochemical determination of serotonin in urine samples based on metal oxide nanoparticles/MWCNT on modified glassy carbon electrode, *Sensing and Bio-Sensing Research* **13** (2017) 17-27. <https://doi.org/10.1016/j.sbsr.2017.01.005>
- [22] H. Beitollahi, S. Tajik, F. Garkani Nejad, Utilization of MoS<sub>2</sub> nanosheets/MnO<sub>2</sub> nanorods-based electrochemical sensor for 4-aminophenol determination in the presence of acetaminophen, *Journal of Environmental Chemical Engineering* **13** (2025) 117113. <https://doi.org/10.1016/j.jece.2025.117113>
- [23] A. Jirasirichote, E. Punrat, A. Suea-Ngam, O. Chailapakul, S. Chuanuwatanakul, Voltammetric detection of carbofuran determination using screen-printed carbon electrodes modified with gold nanoparticles and graphene oxide, *Talanta* **175** (2017) 331-337. <https://doi.org/10.1016/j.talanta.2017.07.050>
- [24] W. Kit-Anan, A. Olarnwanich, C. Sriprachuabwong, C. Karuwan, A. Tuantranont, A. Wisitsoraat, A. Pimpin, Disposable paper-based electrochemical sensor utilizing inkjet-printed Polyaniline modified screen-printed carbon electrode for Ascorbic acid detection, *Journal of Electroanalytical Chemistry* **685** (2012) 72-78. <https://doi.org/10.1016/j.jelechem.2012.08.039>
- [25] S. Tajik, Z. Dourandish, F. Garkani Nejad, A. Aghaei Afshar, H. Beitollahi, Voltammetric determination of isoniazid in the presence of acetaminophen utilizing MoS<sub>2</sub>-nanosheet-modified screen-printed electrode, *Micromachines* **13** (2022) 369. <https://doi.org/10.3390/mi13030369>
- [26] M. F. Bergamini, D. P. Santos, M. V. B. Zanoni, Determination of isoniazid in human urine using screen-printed carbon electrode modified with poly-L-histidine, *Bioelectrochemistry* **77** (2010) 133-138. <https://doi.org/10.1016/j.bioelechem.2009.07.010>
- [27] S. H. Huang, H. H. Liao, D. H. Chen, Simultaneous determination of norepinephrine, uric acid, and ascorbic acid at a screen printed carbon electrode modified with polyacrylic acid-coated multi-wall carbon nanotubes, *Biosensors and Bioelectronics* **25** (2010) 2351-2355. <https://doi.org/10.1016/j.bios.2010.03.028>

- [28] M. R. Ganjali, F. Garkani Nejad, H. Beitollahi, S. Jahani, M. Rezapour, B. Larijani, Highly sensitive voltammetric sensor for determination of ascorbic acid using graphite screen printed electrode modified with ZnO/Al<sub>2</sub>O<sub>3</sub> nanocomposite, *International Journal of Electrochemical Science* **12** (2017) 3231-3240. <https://doi.org/10.20964/2017.04.07>
- [29] S. Tang, A. Liang, M. Liu, W. Wang, F. Zhang, A. Luo, A glassy carbon electrode modified with a composite consisting of electrodeposited chitosan and carboxylated multi-walled carbon nanotubes for simultaneous voltammetric determination of dopamine, serotonin and melatonin, *Carbon Letters* **33** (2023) 2129-2139. <https://doi.org/10.1007/s42823-023-00556-6>
- [30] K. Shekher, K. Sampath, S. Vandini, M. Satyanarayana, K. V. Gobi, Gold nanoparticle assimilated polymer layer on carbon nanotube matrices for sensitive detection of serotonin in presence of dopamine in-vitro, *Inorganica Chimica Acta* **549** (2023) 121399. <https://doi.org/10.1016/j.ica.2023.121399>
- [31] R. Mondal, B. Show, S. F. Ahmed, N. Mukherjee, Electrochemically selective detection of dopamine over serotonin by CuO/Cu<sub>2</sub>O bulk heterostructure electrode, *Bulletin of Materials Science* **47** (2024) 62. <https://doi.org/10.1007/s12034-023-03131-x>
- [32] Z. Dourandish, Z. Ghasemi, MOF/MWCNTs nanocomposite modified glassy carbon electrode for voltammetric determination of sulfanilamide, *Advanced Journal of Nanochemistry and Medicine* **1** (2025) 52-62. <https://doi.org/10.48309/ajn.2025.533392.1003>
- [33] Z. Li, X. Zhang, Y. Luo, Q. Li, Y. Qin, G. Wang, Z. Liu, An electrochemical sensor based on the composite UiO-66-NH<sub>2</sub>/rGO for trace detection of Pb (II) and Cu (II), *Chemical Physics Letters* **830** (2023) 140825. <https://doi.org/10.1016/j.cplett.2023.140825>
- [34] H. Liang, M. Zhu, H. Ye, C. Zeng, S. Wang, Y. Niu, Carbon fiber microelectrode array loaded with the diazonium salt-single-walled carbon nanotubes composites for the simultaneous monitoring of dopamine and serotonin in vivo, *Analytica Chimica Acta* **1186** (2021) 339086. <https://doi.org/10.1016/j.aca.2021.339086>
- [35] F. Garkani Nejad, H. Beitollahi, Voltammetric determination of tert-butylhydroquinone in the presence of butylated hydroxyanisole using 2D Ni-MOF nanosheets/MWCNTs-based electrochemical sensor, *Microchemical Journal* **216** (2025) 114539. <https://doi.org/10.1016/j.microc.2025.114539>
- [36] J. Liu, L. Zhang, H. Ma, H. Sun, S. A. Ge, J. Liu, C. Quan, Quaternary ammonium chitosan-functionalized mesoporous silica nanoparticles: A promising targeted drug delivery system for the treatment of intracellular MRSA infection, *Carbohydrate Polymers* **352** (2025) 123184. <https://doi.org/10.1016/j.carbpol.2024.123184>
- [37] L. Lv, Y. Li, J. Tang, F. Zhang, Ag/TiO<sub>2</sub> photocatalytic synergistic persulfate activation for degradation of methyl orange, *Optical Materials* **159** (2025) 116600. <https://doi.org/10.1016/j.optmat.2024.116600>
- [38] F. Mirzaee Rad, F. Tafvizi, H. Noorbazargan, A. Iranbakhsh, Ag-doped ZnO nanoparticles synthesized through green method using Artemisia turcomanica extract induce cytotoxicity and apoptotic activities against AGS cancer cells: an in vitro study, *Journal of Nanostructure in Chemistry* **14** (2024) 403-418. <https://doi.org/10.1007/s40097-023-00528-2>
- [39] H. Beitollahi, F. Garkani Nejad, S. Z. Mohammadi, S. Tajik, A novel electrochemical sensing platform based on Zn-Co ZIFs/GO nanocomposite and ionic liquid for sensitive determination of methotrexate in the presence of calcium folinate, *Journal of The Electrochemical Society* **172** (2025) 106503. <https://doi.org/10.1149/1945-7111/ae09ff>
- [40] H. Kim, Y. Jung, W. Lee, Y. P. Jeon, J. Y. Hong, J. U. Lee, Sustainable MXene synthesis via molten salt method and nano-silicon coating for enhanced lithium-ion battery performance, *Molecules* **30** (2025) 812. <https://doi.org/10.3390/molecules30040812>

- [41] A. Herawati, R. M. Aryani, G. Antarnusa, A. Nene, Fe<sub>3</sub>O<sub>4</sub>/chitosan nanocomposites for Congo red removal: adsorption surpasses photodegradation, *Materials Chemistry and Physics* **347** (2025) 131431. <https://doi.org/10.1016/j.matchemphys.2025.131431>
- [42] S. Shahrokhian, L. Naderi, M. Ghalkhani, Modified glassy carbon electrodes based on carbon nanostructures for ultrasensitive electrochemical determination of furazolidone, *Materials Science and Engineering C* **61** (2016) 842-850. <https://doi.org/10.1016/j.msec.2016.01.025>
- [43] S. Mirzaei, L. LotfiKatooli, A. Ahmadpour, M. N. Shahrak, M. R. Haghbin, A. Arami-Niya, Enhancing energy carrier gas storage: Novel MOF-decorated carbons with high affinity toward methane and hydrogen, *Chemical Engineering Research and Design* **203** (2024) 419-430. <https://doi.org/10.1016/j.cherd.2024.01.049>
- [44] Y. Li, Y. Shen, Y. Zhang, T. Zeng, Q. Wan, G. Lai, N. Yang, A UiO-66-NH<sub>2</sub>/carbon nanotube nanocomposite for simultaneous sensing of dopamine and acetaminophen, *Analytica Chimica Acta* **1158** (2021) 338419. <https://doi.org/10.1016/j.aca.2021.338419>
- [45] Y. Ji, W. Li, Y. You, G. Xu, In situ synthesis of M (Fe, Cu, Co and Ni)-MOF@MXene composites for enhanced specific capacitance and cyclic stability in supercapacitor electrodes, *Chemical Engineering Journal* **496** (2024) 154009. <https://doi.org/10.1016/j.cej.2024.154009>
- [46] X. Zhang, C. Gao, L. Li, X. Yan, N. Zhang, J. Bao, Fe based MOF encapsulating triethylenediamine cobalt complex to prepare a FeN<sub>3</sub>-CoN<sub>3</sub> dual-atom catalyst for efficient ORR in Zn-air batteries, *Journal of Colloid and Interface Science* **676** (2024) 871-883. <https://doi.org/10.1016/j.jcis.2024.07.176>
- [47] C. R. Marshall, S. A. Staudhammer, C. K. Brozek, Size control over metal-organic framework porous nanocrystals, *Chemical Science* **10** (2019) 9396-9408. <https://doi.org/10.1039/C9SC03802G>
- [48] A. Hashemi, D. Aliasgari, H. Abbasi, F. Baghbani-Arani, Synthesis and Application of Zr MOF UiO-66 Decorated with Folic Acid-Conjugated Poly Ethylene Glycol as a Strong Nanocarrier for the Targeted Drug Delivery of Epirubicin, *Journal of Cluster Science* **36** (2025) 51. <https://doi.org/10.1007/s10876-025-02768-4>
- [49] P. Mhetar, N. Kale, J. Pantwalawalkar, S. Nangare, N. Jadhav, Metal-organic frameworks: Drug delivery applications and future prospects, *ADMET and DMPK* **12** (2024) 27-62. <https://doi.org/10.5599/admet.2057>
- [50] A. D. Pournara, G. D. Tarlas, G. S. Papaefstathiou, M. J. Manos, Chemically modified electrodes with MOFs for the determination of inorganic and organic analytes via voltammetric techniques: a critical review, *Inorganic Chemistry Frontiers* **6** (2019) 3440-3455. <https://doi.org/10.1039/C9QI00965E>
- [51] X. Lu, K. Jayakumar, Y. Wen, A. Hojjati-Najafabadi, X. Duan, J. Xu, Recent advances in metal-organic framework (MOF)-based agricultural sensors for metal ions: a review, *Microchimica Acta* **191** (2024) 58. <https://doi.org/10.1007/s00604-023-06121-2>
- [52] K. Karami, A. Mardaniboldaji, M. R. Rezayat, P. Bayat, M. T. Jafari, Novel UiO-66-NH<sub>2</sub>/Gly/GO Nanocomposite Adsorbent for Ultra-trace Analyzing of Chlorpyrifos Pesticide by Ion Mobility Spectrometry, *ChemistrySelect* **6** (2021) 3370-3377. <https://doi.org/10.1002/slct.202004535>
- [53] Z. Li, X. Zhang, Y. Luo, Q. Li, Y. Qin, G. Wang, Z. Liu, An electrochemical sensor based on the composite UiO-66-NH<sub>2</sub>/rGO for trace detection of Pb (II) and Cu (II), *Chemical Physics Letters* **830** (2023) 140825. <https://doi.org/10.1016/j.cplett.2023.140825>
- [54] Y. Li, Y. Shen, Y. Zhang, T. Zeng, Q. Wan, G. Lai, N. Yang, A UiO-66-NH<sub>2</sub>/carbon nanotube nanocomposite for simultaneous sensing of dopamine and acetaminophen, *Analytica Chimica Acta* **1158** (2021) 338419. <https://doi.org/10.1016/j.aca.2021.338419>
- [55] X. Yao, J. Shen, Q. Liu, H. Fa, M. Yang, C. Hou, A novel electrochemical aptasensor for the sensitive detection of kanamycin based on UiO-66-NH<sub>2</sub>/MCA/MWCNT@rGONR

- nanocomposites, *Analytical Methods* **12** (2020) 4967-4976.  
<https://doi.org/10.1039/D0AY01503B>
- [56] Q. Chen, X. Li, X. Min, D. Cheng, J. Zhou, Y. Li, C. Zhang, Determination of catechol and hydroquinone with high sensitivity using MOF-graphene composites modified electrode, *Journal of Electroanalytical Chemistry* **789** (2017) 114-122.  
<https://doi.org/10.1016/j.jelechem.2017.02.033>
- [57] F. Ebrahimi-Tazangi, J. Seyed-Yazdi, H. Fe<sub>3</sub>O<sub>4</sub>-NH<sub>2</sub>/GO an effective modifier for simultaneous voltammetric detection of isoniazid in the presence of acetaminophen, *Advanced Journal of Nanochemistry and Medicine* **1** (2025) 30-51.  
<https://doi.org/10.48309/ajnm.2025.531917.1000>
- [58] K. S. Postolović, M. B. Radovanović, Z. D. Stanić, Simultaneous determination of serotonin, dopamine, and ascorbic acid at a glassy carbon electrode modified with chitosan-alginate hydrogel and reduced graphene oxide, *Journal of Electroanalytical Chemistry* **980** (2025) 118992. <https://doi.org/10.1016/j.jelechem.2025.118992>
- [59] R. Zaimbashi, A. Mohammadnavaz, Voltammetric detection of tert-butylhydroquinone Through the Modification of Carbon Paste Electrode with Graphene oxide/Co<sub>3</sub>O<sub>4</sub> nanocomposite, *Journal of Environmental and Bioanalytical Electrochemistry* **2** (2026) 38-48.  
<https://doi.org/10.48309/jebe.2026.532422.1029>
- [60] J. Hong, S. J. Park, S. Kim, Synthesis and electrochemical characterization of nanostructured Ni-Co-MOF/graphene oxide composites as capacitor electrodes, *Electrochimica Acta* **311** (2019) 62-71. <https://doi.org/10.1016/j.electacta.2019.04.121>
- [61] S. Tajik, P. Shams, H. Beitollahi, F. Garkani Nejad, Electrochemical nanosensor for the simultaneous determination of anticancer drugs epirubicin and topotecan using UiO-66-NH<sub>2</sub>/GO nanocomposite modified electrode, *Biosensors* **14** (2024) 229.  
<https://doi.org/10.3390/bios14050229>